## INVESTIGATING THE NON-FLOW EFFECTS OF LONG-LIVED STABLE HADRONS IN PROTON+PROTON COLLISIONS AT LHC ENERGIES USING PYTHIA8

M.Sc. Thesis

By

#### Bendangkokba R Jamir



# DEPARTMENT OF PHYSICS INDIAN INSTITUTE OF TECHNOLOGY INDORE June 2022

### INVESTIGATING THE NON-FLOW EFFECTS OF LONG-LIVED STABLE HADRONS IN PROTON+PROTON COLLISIONS AT LHC ENERGIES USING PYTHIA8

#### A THESIS

Submitted in partial fulfillment
of the requirements for the award of the degree
of

Master of Science

by

Bendangkokba R Jamir

under the guidance of

Prof. Raghunath Sahoo



# DEPARTMENT OF PHYSICS INDIAN INSTITUTE OF TECHNOLOGY INDORE ${\bf June~2022}$



#### INDIAN INSTITUTE OF TECHNOLOGY INDORE

#### CANDIDATE'S DECLARATION

I hereby certify that the work which is being presented in the thesis entitled "INVESTIGATING THE NON-FLOW EFFECTS OF LONG-LIVED STABLE HADRONS IN PROTON+PROTON COLLISIONS AT LHC ENERGIES USING PYTHIA8" in the partial fulfillment of the requirements for the award of the degree of MASTER OF SCIENCE and submitted in the Department of Physics, Indian Institute of Technology Indore, is an authentic record of my own work carried out during the time period from July 2021 to June 2022 under the supervision of Prof. Raghunath Sahoo, Professor, Indian Institute of Technology Indore.

The matter presented in this thesis has not been submitted by me for the award of any other degree of this or any other institute.

(Bendangkokba R Jamir)

This is to certify that the above statement made by the candidate is correct to the best of my knowledge.

Dr. Raghunath Sahoo | वॉ. रघुनाथ साह् Professor | आध्यापक Department of Physics | गौतिकी विषाय Indian Institute of Technology Indore, India

(Prof. Raghunath Sahoo)

Bendangkokba R Jamir has successfully given his M.Sc. Oral Examination held on June 07, 2022.

(M.Sc Thesis Supervisor)

Date:

Marrenda

(PSPC Member 1)
Date:

(Convener, DPGC)

Nate:

(PSPC Member 2)

Date:

#### ACKNOWLEDGEMENT

First and foremost, praises and thanks to God, the Almighty, for His showers of blessings throughout my research work to complete the thesis successfully. I would like to express my deep and sincere gratitude to my thesis supervisor, Prof. Raghunath Sahoo, for allowing me to work under him and providing invaluable guidance throughout my research. It was a great privilege and honor to work and study under his guidance. I am extremely grateful for what he has offered me. I would also like to thank him for his friendship, empathy, and great sense of humor.

It goes without saying that I am extremely grateful to my lab members, Mr. Bhagyarathi Sahoo, Dr. Captain Rituraj Singh, Mr. Debadatta Behera, Mr. Dushmanta Sahu, Mr. Girija Sankar Pradhan, Mr. Kamaljeet Singh, Mr. Kshitish Kumar Pradhan, Mr. Neelkamal Mallick, Mr. Ronald Scaria and Mr. Suraj Prasad for their unwavering support and guidance throughout my research. They've all helped me so much that each one deserves credit of their own, but there's one person in particular to whom I owe my deepest gratitude - Suman Deb, my senior and my second mentor, who has been like a brother to me. His dynamism, vision, sincerity, and motivation have all left an indelible impression on me. He taught me the methodology for conducting research and presenting the findings as clearly as possible.

I would like to thank my PSPC members Dr. Dipankar Das and Dr. Manavendra Mahato for their support and insightful comments. I would like to acknowledge the Department of Physics of IIT Indore for providing the necessary resources to carry out this research.

I am extremely grateful to my parents and siblings for their love, prayers, care, and sacrifices in educating and preparing me for my future. My special thanks go to my friends for their constant moral support throughout my research work.

Finally, my thanks go to all the people who have supported me to complete the research work directly or indirectly.

 $\begin{tabular}{ll} Dedicated to my family \\ and \\ Members of the EHEP lab \\ \end{tabular}$ 

#### ABSTRACT

Traditionally proton+proton (pp) collision was considered to be the baseline in measurement for heavy-ion collisions. However, recent studies at the LHC suggest hints of collectivity in small systems, in tandem with strangeness enhancement and ridge-like structure at high multiplicity pp events. This indicates towards the possible formation of a medium even in small systems like that is produced in pp collisions. During ultrarelativisite heavy-ion collisions, the system achieves a very large energy density ( $\epsilon_c > 1~GeV/fm^3$ ) and high temperature (150-170 MeV, which is  $10^5$  hotter than the core of the sun), as a result of which quarks and gluons undergo multiple interactions. These interactions leads to a collective expansion and cooling of particles before they eventually hadronize. This expansion is called "flow". However, this characteristic signal is not only generated by flow; there are also contributions that can mimic flow-like effects. These are referred to as "non-flow". In small collision systems, these non-flow effects are more dominant than in large collision systems (e.g.,lead+lead (Pb+Pb), gold+gold (Au+Au). Thus non-flow effects in small systems needs to be studied in detail to have a better understanding of the dynamics of the system, With this motivation, in this work we have investigated the contribution of non-flow effects in pp system by long-lived hadrons at  $\sqrt{s}=13$  TeV and 7 TeV using pQCD inspired model (PYTHIA8). We have extracted elliptic flow by virtue of non-flow effects and relative associated yield to have an idea about medium effects in pp system.

# Contents

1	Intr	roduction	1
	1.1	Quantum Chromodynamics	2
	1.2	Proton+Proton Collisions	4
	1.3	Relativistic Kinematics	5
		1.3.1 Rapidity and Pseudorapidity	5
		1.3.2 Azimuthal and Polar Angles	7
		1.3.3 Choice of Units	8
	1.4	Flow and Non-flow effects	9
	1.5	Charged Multiplicity	11
	1.6	Thesis Goals	12
2	Mo	tivation and Analysis tools	13
	2.1	PYTHIA8: Event Generator	14
		2.1.1 Multi-Partonic Interaction (MPI)	15

		2.1.2 Color Reconnection (CR)	15
	2.2	ROOT Framework	16
3	Two	particle Azimuthal Correlation	19
	3.1	Event generation and Analysis methodology	22
4	Ana	alysis and Discussion	23
	4.1	Mean Transverse Momentum and Charged-Particle Mul-	
		tiplicity	23
	4.2	Two-dimensional $(\Delta \eta - \Delta \phi)$ correlation distribution	26
	4.3	One-dimensional $(\Delta \phi)$ correlation function	31
	4.4	Estimation of flow-like effects	33
	4.5	Extraction of relative associated yields	35
5	Sun	nmary and Outlook	37

# List of Figures

1.1	Standard Model of elementary particles [1]	2
1.2	QCD phase diagram [2]	3
1.3	Pseudorapidity of particles corresponding to different polar angles [5]	7
1.4	Representation of detector geometry [6]	7
1.5	After a non-central collision of two heavy-ion nuclei, the interaction volume has an almond shape [7]	10
1.6	Charged-Particle Multiplicity Distribution $(N_{ch})$ in pp collisions at $\sqrt{s}=13$ TeV using PYTHIA8	11
4.1	(Color Online) (Top) Mean Transverse momentum $< p_{\rm T} > {\rm vs}~N_{ch}$ (Bottom) Charged Multiplicity distribution for pp collision at $\sqrt{s}$ =13 TeV and 7 TeV	24
4.2	(Color Online) number of Multi Partonic Interaction $(n_{MPI})$ vs $N_{ch}$ . We can see that $n_{MPI}$ gets saturated at high multiplicity	25

- 4.3 (Color Online) Column (I) Correlation distributions for same event, Column (II) Correlation distributions for mixed events, Column (III) Ratio of same event correlation distribution to mixed event correlation distribution for low multiplicity (Mult.Class: 1) at  $\sqrt{s} = 13$  TeV for Pion  $(\pi^{\pm})$  [Row(I)], Kaon $(k^{\pm})$  [Row(II)] and Proton [Row(III)] 27
- 4.4 (Color Online) Column (I) Correlation distributions for same event, Column (II) Correlation distributions for mixed events, Column (III) Ratio of same event correlation distribution to mixed event correlation distribution for high multiplicity (Mult.Class: 6) at  $\sqrt{s} = 13$  TeV for Pion  $(\pi^{\pm})$  [Row(I)], Kaon( $k^{\pm}$ ) [Row(II)] and Proton [Row(III)] 28
- 4.5 (Color Online) Column (I) Correlation distributions for same event, Column (II) Correlation distributions for mixed events, Column (III) Ratio of same event correlation distribution to mixed event correlation distribution for low multiplicity (Mult.Class: 1) at  $\sqrt{s} = 7$  TeV for Pion ( $\pi^{\pm}$ ) [Row(I)], Kaon( $k^{\pm}$ ) [Row(II)] and Proton [Row(III)] . . . 29
- 4.6 (Color Online) Column (I) Correlation distributions for same event, Column (II) Correlation distributions for mixed events, Column (III) Ratio of same event correlation distribution to mixed event correlation distribution for high multiplicity (Mult.Class: 6) at  $\sqrt{s} = 7$  TeV for Pion ( $\pi^{\pm}$ ) [Row(I)], Kaon( $k^{\pm}$ ) [Row(II)] and Proton [Row(III)] . . 30

4.7	Uncorrected 1-D Correlation Distribution of proton for	
	two multiplicity classes. As we can see, the baseline for	
	the two multiplicity classes in comparison is not same .	31
4.8	(Color Online) Column (I) Corrected 1-D Correlation Dis-	
	tribution for Min. Bias, Column (II) Corrected 1-D Cor-	
	relation Distribution for low multiplicity (Mult. Class:	
	1), Column (III) Corrected 1-D Correlation Distribution	
	for high multiplicity (Mult.Class: 6)	32
4.9	(Color Online) Row (I) Fitted correlation distributions	
	for $\pi^{\pm}$ , $k^{\pm}$ , $p+\bar{p}$ for low multiplicity class and Row (II)	
	for high multiplicity class	33
4.10	(Color Online) $v_2$ vs. $N_{ch}$ for $\pi^{\pm},k^{\pm},\mathrm{p}{+}\bar{p}$	34
4.11	(Color Online) $I_{pp}$ vs. $N_{ch}$ for $\pi^{\pm}, k^{\pm}, p+\bar{p}$	36



# List of Tables

4.1	Event multiplicity classes used in the analysis. It may be	
	noted here that the analysis has been performed within	
	midrapidity range $ \eta  < 1$	25

# Chapter 1

### Introduction

"...all of biology can be summarized in the language of chemistry, all of chemistry can be summarized in the language of physics...." - Dr. Michio Kaku, theoretical physicists, City College of New York.

The known matter in the universe is made up of atoms, and atoms are made up of nucleus/nucleons surrounded by a cloud of leptons called electrons. The nucleus, is further composed of protons and neutrons. Upon further peeking into the protons and neutrons, we see that they composed of elementary particles called quarks and gluons. The Standard Model, developed during the later half of the 20<sup>th</sup> century, describes these fundamental particles (Figure 1.1) and their interactions with the three fundamental forces - electromagnetic, weak and strong nuclear force (Standard Model does not reconcile gravity).

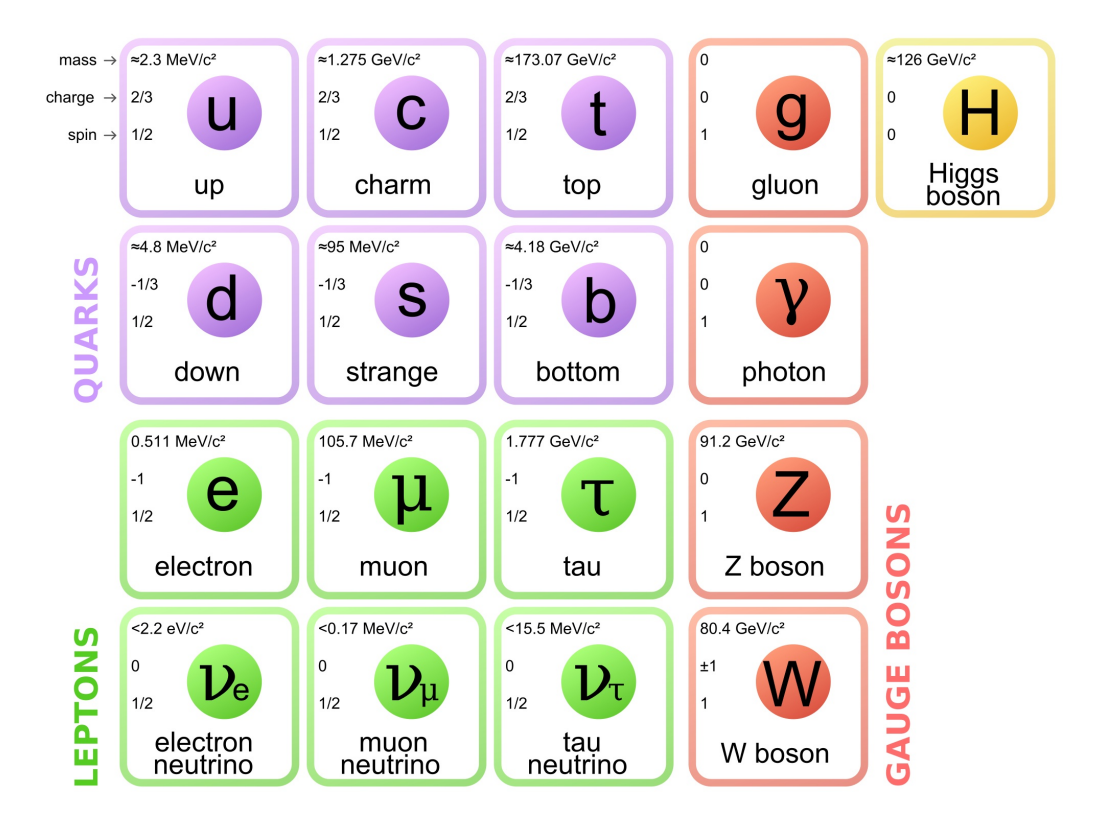


Figure 1.1: Standard Model of elementary particles [1]

#### 1.1 Quantum Chromodynamics

Quantum Chromodynamics (QCD), the theory of strong interaction describes the strong nuclear force. The QCD potential between partons can be written as:

$$V(r) = -\frac{4}{3}\frac{\alpha_s}{r} + kr \tag{1.1}$$

where  $\alpha_s$  is the coupling strength of strong interaction, k is the spring tension and r is the distance between two quarks. When the distance is large  $(r \gg 1 \text{ fm})$ , the second term of equation 1.1 will dominate the potential function. This describes the property of confinement, which requires the quarks and gluons to be confined in hadrons. When the distance is small ( $r \ll 1 \text{ fm}$ ), the quarks exchange fewer gluons and the net force becomes weaker and thus the quarks are relatively free.

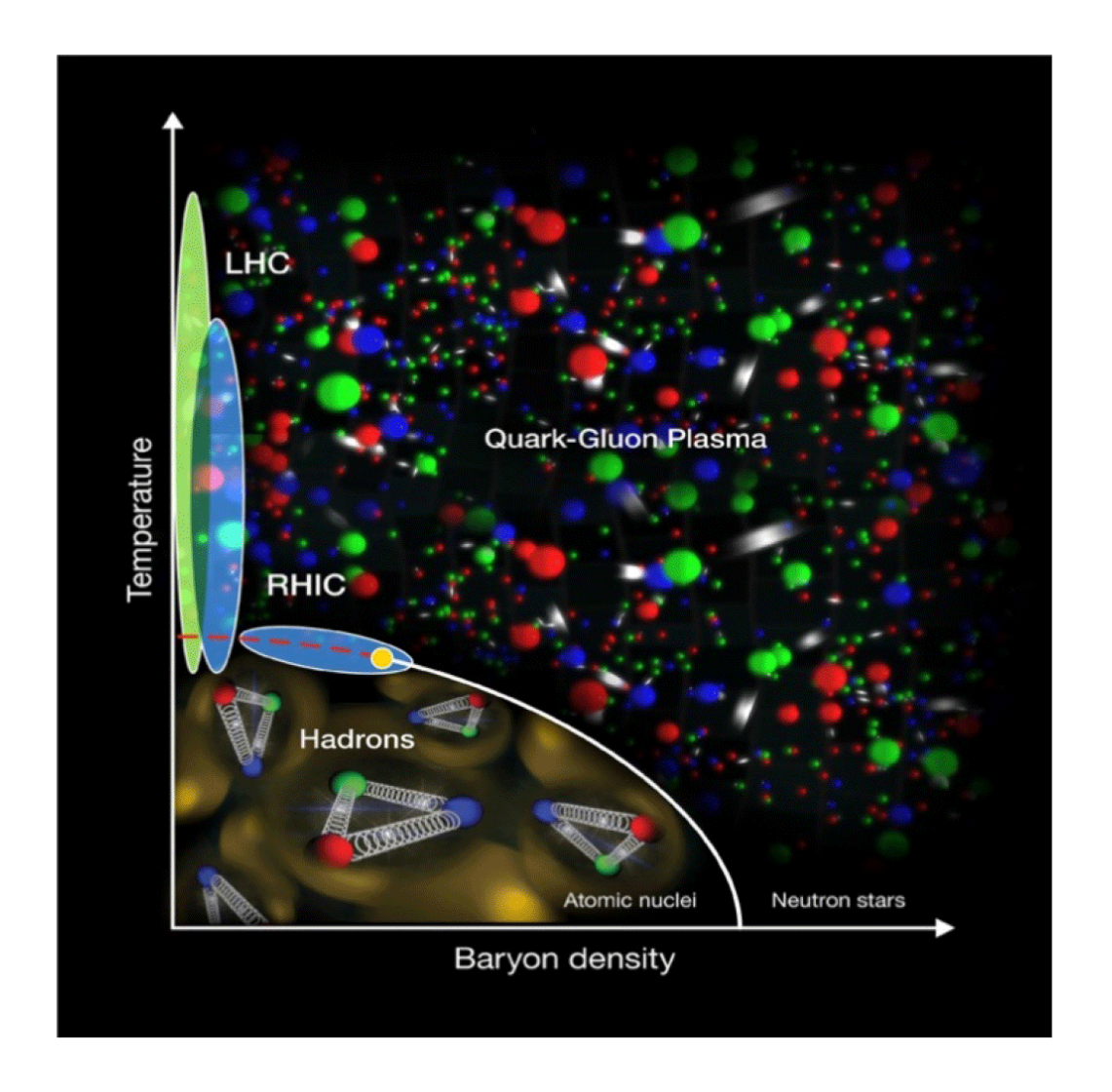


Figure 1.2: QCD phase diagram [2]

This property of quarks is known as asymptotic freedom. Lattice QCD predicts the formation of a partonic (quarks and gluons) state at high temperature (T) and/or at high bayron chemical potential  $(\mu_B)$ . This outrageous state of affair is a new state of matter called **Quark Gluon Plasma (QGP)**. Thus, QGP is defined as a (locally) thermally equilibrated system where the partons are deconfined from the hadrons [3]. QGP can be achieved by two ways - either by heating the nuclei to ultra-high temperature as is done at the Relativistic Heavy Ion Collider (RHIC) and at the Large Hadron Collider (LHC), or by compressing the nuclei so as to diffuse the hadronic boundaries; this experiment is

expected to be carried out at the Facility for Antiproton and Ion Research (FAIR) at GSI, Germany and the Nuclotron-based Ion Collider facility (NICA), Joint Institute for Nuclear Research (JINR), Russia [3]. From the QCD phase diagram (Figure 1.2), high temperature and low  $\mu_B$  corresponds to an early Universe scenario, whereas low temperature and high  $\mu_B$  regime corresponds to different astrophysical objects like neutron stars. At low bayron density  $\mu_B$ , there is a smooth crossover from the hadronic to the QGP phase. However, at higher  $\mu_B$ , there exists a  $1^{st}$  order phase transition line, which ends with a possible critical point (shown as a yellow dot in Figure 1.2), after which the phase transition is a cross-over. Thus, when nuclear matter is subjected to very high energy densities and high temperatures, the nuclear matter achieves QGP state, where quarks and gluons are no longer bound in individual hadrons. In the present day, high energy physicists study QCD interactions over a wide range of energies (from several GeV to TeV). This is primarily achieved by colliding heavy ions. However, recent studies at RHIC and LHC energies shows the possible formation of QGP at high multiplicity pp collisions as well. Hence, the quest to search for QGP has been at the frontier in the field of high energy nuclear physics.

#### 1.2 Proton+Proton Collisions

It is crucial to understand the underlying mechanism of pp collisions, as proton is the lightest bayron. A pp collision can simple be considered as two point particles colliding. But at higher energies, the same point

particles becomes a distribution of partons and hence we observe a direct collisions between the partons. The whole analysis in this thesis has been done for pp collisions at LHC energies.

#### 1.3 Relativistic Kinematics

The particles studied in particle physics are treated relativistically and hence Special Theory of Relativity (STR) becomes important in describing the particle kinematics. Albert Einstein's Special Theory of Relativity has the following two underlying assumptions:

- The speed of light c remains constant in all *inertial frame* regardless of the motion of the observer or source.
- The laws of physics are the same in all inertial frame of references.

  Mathematically, it means that the physical laws need to be expressed in Lorentz tensors.

#### 1.3.1 Rapidity and Pseudorapidity

In the relativistic domain, velocity is not additive in nature *i.e* non-linear in successive Lorentz transformations. Thus, velocity is not a good choice of kinematic variable for studying relativistic particles. In order to circumvent this drawback, we introduce a new kinematic variable called *rapidity*. It is a dimensionless quantity and is defined as the ratio of the forward light cone momentum  $(p_+)$  to the backward

light cone momentum  $(p_{-})$  [4]. Mathematically it can be expressed as:

$$y = \frac{1}{2} \ln \frac{p_{+}}{p_{-}} = \frac{1}{2} \ln \frac{E + p_{z}c}{E - p_{z}c}$$
 (1.2)

where E and  $p_z$  are the energy and z-component of the particle's momentum. One can show rapidity to be an additive quantity *i.e.* y'' = y + y'. Thus, rapidity changes by an additive constant under successive Lorentz boosts [4]. Now, equation 1.2 can be re-written as

$$y = \frac{1}{2} \ln \frac{(p^2 c^2 + m^2 c^4)^{1/2} + p_z c}{(p^2 c^2 + m^2 c^4)^{1/2} - p_z c}$$
(1.3)

Simplifying further and taking the first few terms of Binomial expansion series we get

$$y \simeq \frac{1}{2} \ln \frac{1 + \frac{p_z}{p} + \frac{m^2 c^4}{2p^2 c^2 + \dots}}{1 - \frac{p_z}{p} + \frac{m^2 c^4}{2p^2 c^2 + \dots}}$$
(1.4)

we know that for relativistic particles,  $pc \gg mc^2$ . Thus equation 1.4 reduces to

$$y \simeq \frac{1}{2} \ln \frac{1 + \cos(\theta)}{1 - \cos(\theta)} = -\ln \tan \frac{\theta}{2}$$
 (1.5)

We define pseudorapidity  $(\eta)$  as

$$\eta = -\ln \tan \frac{\theta}{2} \tag{1.6}$$

For relativistic particles  $\eta \simeq y$ . The advantage of using pseudorapidity over rapidity for collider experiments is that one needs to know only  $\theta$  *i.e.* the particle trajectory angle with the beam axis for estimation rather than to estimate energy and z-component of momentum which in turn necessitates to know the particle identification (mass).

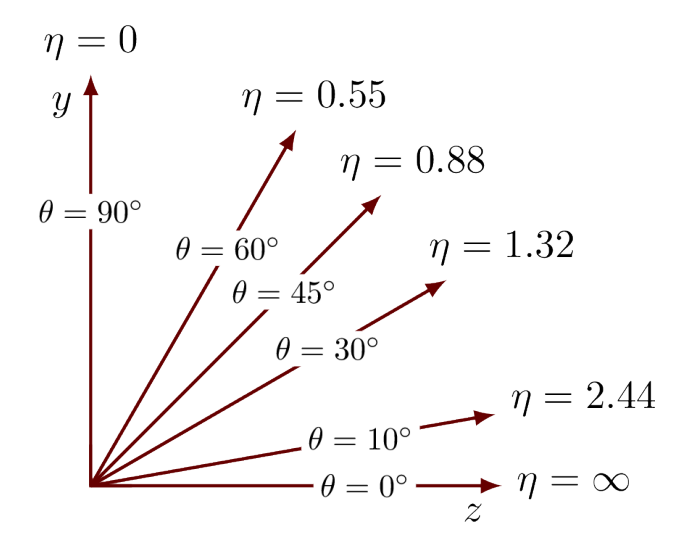


Figure 1.3: Pseudorapidity of particles corresponding to different polar angles [5]

#### 1.3.2 Azimuthal and Polar Angles

In the  $(\eta - \phi)$  coordinate system, the azimuthal angle  $\phi$  is defined as

$$\phi = \tan^{-1} \frac{p_y}{p_x} \tag{1.7}$$

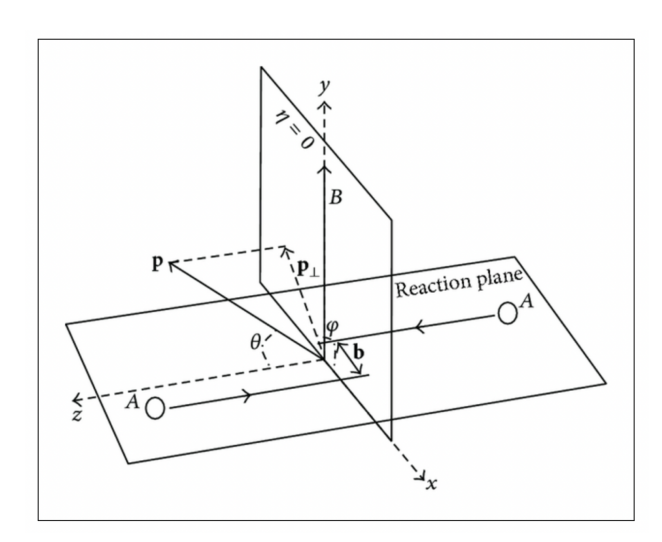


Figure 1.4: Representation of detector geometry [6]

The polar angle  $\theta$  describes the particle trajectory angle w.r.t the beam direction (z-axis). It is defined as

$$\theta = \cos^{-1} \frac{p_z}{|\vec{p}|} = \tan^{-1} \frac{|\vec{p_T}|}{p_z}$$
 (1.8)

Figure 1.4 gives a pictorial representation of detector geometry with z-axis taken as the beam axis, the polar angle  $\theta$  and the azimuthal angle  $\phi$  with the impact parameter b in the reaction plane.

#### 1.3.3 Choice of Units

Since physical constants like the speed of light (c), reduced Planck's constant  $(\hbar)$  and Boltzmann's constant (k) appear frequently in many of the formulas, it quickly becomes cumbersome to write these constants every time in our calculations, thereby making it messy and complicated. Thus, in order to simplify things, we introduce a new system of unit called the natural units and more popularly used in high-energy (particle) physics. In natural units  $\hbar = c = 1$ , where

$$\hbar = \frac{h}{2\pi} = 1.055 * 10^{34} \text{ Joule sec}: (ML^2T^{-1})$$
 $c = 2.998 * 10^8 \text{ meter } sec^{-1}: (LT^{-1})$ 

Thus, in the new unit system, the relativistic energy formula

$$E^2 = p^2 c^2 + m^2 c^4 (1.9)$$

reduces to the simple formula

$$E^2 = p^2 + m^2 (1.10)$$

In particle physics, the unit of energy is GeV (1  $GeV = 10^9 \ eV$ ). This leads us to expressing mass (m) and momentum (mc) in GeV, length  $(\hbar/2\pi)$  and time  $(\hbar/mc^2)$  in  $GeV^{-1}$ .

#### 1.4 Flow and Non-flow effects

During pp collision, due to very large energy density and high temperature of the system, the quarks and gluons (partons) undergo multiple interactions. This dynamical evolution leads to a collective expansion of the system and eventually hadronization. This collective expansion is called flow. Flow describes the variation of energy, momentum and number of particles with direction [7] and indicates the presence of many interactions between the medium's constituents as a result of the collision. It is caused by the initial asymmetries in the geometry of the colliding system. The most direct indication of collective flow is the observation of azimuthal anisotropy in particle production. A clever way to mathematically describe anisotropic flow is to use a Fourier expansion of the invariant triple differential distributions,

$$E\frac{d^3N}{d\mathbf{p}^3} = \frac{d^3N}{p_{\rm T}dp_{\rm T}d\phi dy} \tag{1.11}$$

$$\frac{d^3N}{p_{\rm T}dp_{\rm T}d\phi dy} = \frac{1}{2\pi} \frac{d^2N}{p_{\rm T}dp_{\rm T}d\eta} (1 + 2\sum_{n=1}^{\infty} v_n \cos\left[n(\phi - \Psi_{RP})\right]$$
(1.12)

where E is the energy of the particle, p the momentum,  $p_{\rm T}$  its corresponding transverse momentum,  $\eta$  the pseudorapidity and  $\Psi_{RP}$  the reaction plane. Here  $v_n$  are the anisotropy coefficients. It may be noted here that the sine terms in the expansion vanishes due to reflection symmetry with respect to the reaction plane angle. The Fourier anisotropy coefficients are  $p_{\rm T}$  and  $\eta$  dependent, and are given by,

$$v_n(p_{\mathrm{T}}, \eta) = \langle \cos \left[ n(\phi - \Psi_{RP}) \right] \rangle \tag{1.13}$$

where, the angular brackets denote an average over the particles, summed over all events, in  $(p_T, \eta)$  bin under study. In the decomposition,  $v_1$ ,  $v_2$  and  $v_3$  are known as directed flow, elliptic flow and triangular flow, respectively.

The elliptic flow,  $(v_2)$ , is a crucial observable for analyzing the ef-

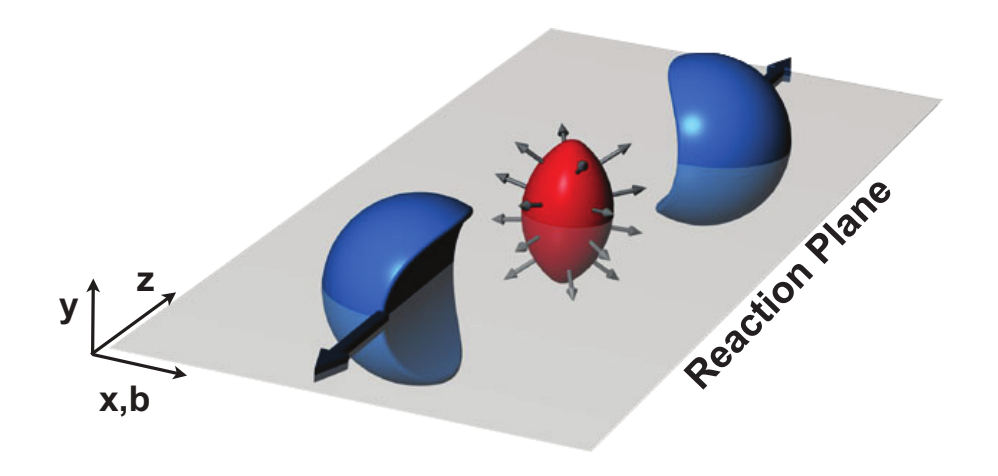


Figure 1.5: After a non-central collision of two heavy-ion nuclei, the interaction volume has an almond shape [7]

fects of the system's initial state and collective expansion. It is a strong evidence of QGP formation and has been described as a paramount observation first at the Relativistic Heavy Ion Collider (RHIC) and later at the Large Hadron Collider [8]. In heavy-ion collisions with non-zero impact parameters, the overlap zone takes on an almond form, as illustrated in Figure 1.5, and a pressure gradient develops, with maximum pressure along the minor axis and minimum pressure along the major axis (beam axis). This initial state spatial anisotropy results in the momentum anisotropy of the final state particles.

However, there are certain characteristics which mimics like flow effects. These imitators are referred to as *non-flow effects*.

Examples of non-flow effects includes resonance decays, jet quenching,

Coulomb interactions, and particle decays. These non-flow effects are insignificant in large collision systems (Pb+Pb, Au+Au), however in small collision systems such as pp system, they are dominant and hence must be well understood in order to extract the real flow signal from the data.

#### 1.5 Charged Multiplicity

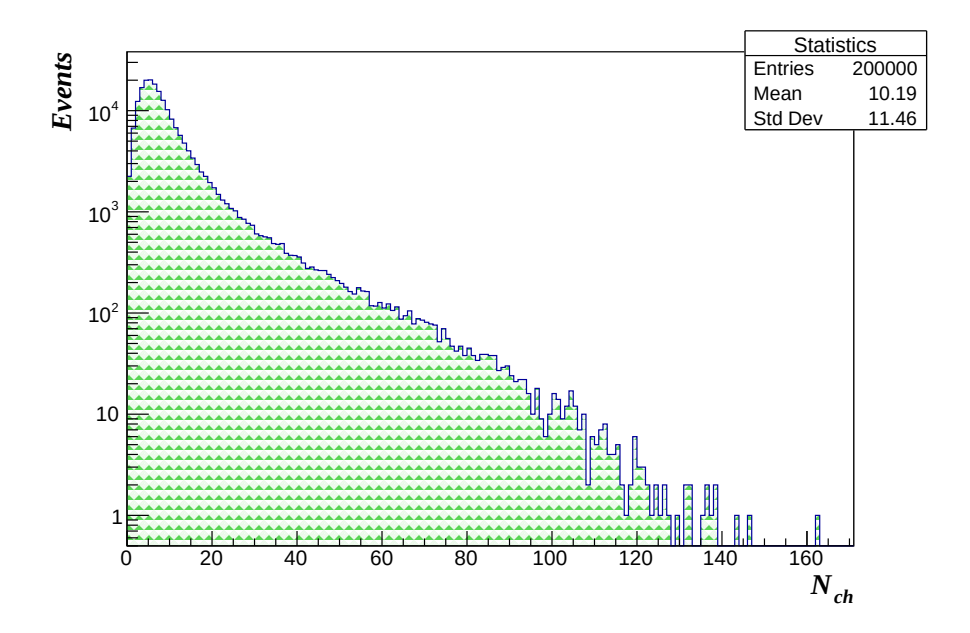


Figure 1.6: Charged-Particle Multiplicity Distribution  $(N_{ch})$  in pp collisions at  $\sqrt{s} = 13$  TeV using PYTHIA8

Charged multiplicity refers to the number of final state particles detected in a collision. Collisions which produces large number of final state particles are referred to as high multiplicity. Such large number of final state particles are produced in central or head-on type of collisions. Whereas, those collisions which produce less number of final state particles are referred to as low multiplicity events. It occurs in the peripheral or non-central type of collisions. Figure 1.6 shows a typical

charged multiplicity distribution, with  $N_{ch}$  i.e. the number of final state charged particles on the x-axis and the probability or the frequency of occurrence of events on the y-axis.

#### 1.6 Thesis Goals

High multiplicity pp collision at LHC energies are gaining a research spotlight in the high energy scientific community nowadays. Many results pertaining to high multiplicity pp collision indicate towards a possible formation of a deconfined medium [9]. One such indication is the anisotropic flow effects. But since non-flow effects can also mimic flowlike effects and moreover, it is dominant in small collision systems such as pp system, it must be well investigated. In this thesis, we present the calculation of  $v_2$  by two particle azimuthal correlation formalism using PYTHIA8, a Monte Carlo event generator. Since PYTHIA does not incorporate QGP medium in its model, one should not observe any flowlike effects. The presence of a finite  $v_2$  indicates the presence of various underlying events which attribute to the non-flow effects. This thesis is organised as follows: Chapter 2 talks about the motivation behind the project and the analysis tools used - ROOT (v6.25/01) and PYTHIA8 (v8.306). Chapter 3 explains the formalism used for the analysis. In chapter 4, we analyse and present the various results obtained and finally in chapter 5 we conclude the thesis by presenting an overview summary of the work and outlines the future outlook.

# Chapter 2

# Motivation and Analysis tools

The possible formation of a deconfined medium at high multiplicity ppcollisions has gained an immense spotlight and an area of intense research for the scientific community. At the onset on such enthralling times for pp collisions, addressing the effects of non-flow contribution is of paramount importance, since, these effects are more dominant in small systems such as pp systems. We have investigated the contributions from non-flow effects in pp systems by generating events using a Monte Carlo event generator which does not incorporate the formation of QGP medium in its model, viz., PYTHIA8. The generated data is then analysed using ROOT framework. The formalism used for our analysis is the statistical two particle azimuthal correlation method (detail discussion in chapter 3). Upon plotting the correlation distribution as a function of differences in the azimuthal angle, we observe two Gaussianbell like peaks around  $\Delta \phi = 0$  and around  $\Delta \phi = \pi$ . In the absence of a medium, we expect these two peaks to be of same width and height. Detailed investigation in this thesis shows that the peak around  $\Delta \phi = \pi$ 

is smaller, thereby suggesting that there exists certain underlying events which results in the differences of heights in the two peaks. These underlying events result in the so called non-flow effects, as PYTHIA doesn't incorporate the formation of QGP medium in its model. These non-flow effects attributes to momentum space anisotropy which causes in height differences of the two peaks of the correlation distribution, and this motivates us to investigate further into the the non-flow contributions. For this analysis, we have used two methodological tools. The generation of various events was done using PYTHIA8. In order to extract the data, perform various calculation and plotting the results, we have used ROOT, object-oriented program and library developed at CERN.

#### 2.1 PYTHIA8: Event Generator

PYTHIA8 is a C++ based pQCD inspired Monte Carlo event generator used for generation of high energy physics events in elementary particle collisions [10]. It includes a set of physics models that describe the progression from a few-body hard process to a complicated multihadronic state. The following physics processes are incorporated in Pythia:

- QCD processes Hard and Soft Processes
- Multi Partonic Interaction (MPI)
- Color Reconnection (CR)
- Resonance Decays
- Ordinary Decays of high mass particles

- Initial-state parton Radiation (ISR)
- Final-state parton Radiation (FSR)
- Beam Remnants

#### 2.1.1 Multi-Partonic Interaction (MPI)

Multi-Partonic Interaction (MPI) refers to a large number of interaction occurring amongst the quarks and gluons in a single pp event. Particle production is largely dependent on MPI since several interactions can occur at the partonic level in a single pp collision. One major difference between PYTHIA8 and its predecessor PYTHIA6 is that the MPI is impact parameter dependent for the former, whereas it is independent of the impact parameter for the latter. As a result of which in PYTHIA8, if the initial processes are hard QCD processes, then the subsequent processes are also hard QCD processes. MPI are used for describing underlying events (the sum of all processes that build up the final hadronic state) such as production of gluons, light quarks and production of heavy flavour particles such as  $J/\psi$ , open heavy flavour particles, etc.

#### 2.1.2 Color Reconnection (CR)

In PYTHIA, each quark is considered of as a color tube. Color Reconnection (CR) is a technique of hadronization in PYTHIA in which these color tubes are connected through a color string. These color tubes (quarks) are connected in such a way that their total string length is as short as possible. This ensures for a stable configuration. CR applies

for both soft and hard QCD processes. PYTHIA8 has three different CR models:

- CR(0): This is an MPI-based scheme in which partons from a lower  $p_T$  MPI system are combined with those from a higher  $p_T$  MPI system.
- CR(1): The reconnection probability is calculated using QCD color rules in this model.
- CR(2): This model is based on Gluon motion, in which partons are moved from one location to another to shorten the total string length.

#### 2.2 ROOT Framework

ROOT is an open source data analysis framework developed at CERN. It is used mainly by high energy physicists to analyse the ginormous amounts of data collected from RHIC and LHC, since it enables scientifically accurate analyses and visualization of these large amounts of data. It is an object-oriented framework written mostly in C++ language and can be easily integrated with Python for those users who are more accustomed to Python. ROOT includes a number of powerful mathematical and statistical packages, as well as standard C++ libraries, making it easy for the user to call and use them as needed to extract useful physics information from the data. It uses CINT as its C++ interpreter and gives an interactive environment which enables

users to read and have a visualization of the data through various graphs and histograms [11].

# Chapter 3

# Two particle Azimuthal Correlation

In recent years, the discovery of a long-range ridge-like structure in the near-side region of  $(\Delta \eta - \Delta \phi)$  correlation distribution in high multiplicity pp and p+Pb collisions by CMS and ATLAS experiment at the LHC have generated a lot of interest for researchers to look into the small systems [12]. As mentioned before, the collective expansion of the system can be described by its "flow". But there exists certain characteristics, called non-flow, which mimics flow-like effects. By taking a Monte Carlo event generator such as PYTHIA, which does not incorporate QGP-like medium in its model, the flow-like characteristics thus obtained in our analysis can be considered as purely non-flow effects. So for our analysis, these non-flow effects can be studied through two particle azimuthal correlation formalism.

Two-particle azimuthal correlation is a statistical method in which the properties of "pairs" of particles are studied event-wise. This method measures the correlation between a trigger particle in association with its associated particles in each event, in terms of their differences in

azimuthal angle  $(\Delta \phi)$  and pseudorapidity  $(\Delta \eta)$  [13]. Here, the trigger particle is a particle that decides which event to be recorded, based on certain input parameters and all the other particles associated with this trigger particle are referred to as the associated particles.

The two particle correlation function i.e. associated yield per trigger particle is given by:

$$\frac{1}{N_{trig}} \frac{d^2 N^{pair}}{d(\Delta \eta \Delta \phi)} = B(0, 0) \frac{S(\Delta \eta \Delta \phi)}{B(\Delta \eta \Delta \phi)}$$
(3.1)

where  $N_{trig}$  is the number of trigger particles. Thus, the associated yield per trigger particle can be defined as the number of associated particles obtained in terms of the differences between the trigger and associated particles in the azimuthal angle i.e.  $\Delta \phi = \Delta \phi_{trig} - \Delta \phi_{assoc}$  and pseudorapidity i.e.  $\Delta \eta = \Delta \eta_{trig} - \Delta \eta_{assoc}$  [14].

Here,  $S(\Delta \eta \Delta \phi)$  is given as:

$$S(\Delta \eta \Delta \phi) = \frac{1}{N_{trig}} \frac{d^2 N_{same}^{pair}}{d(\Delta \eta \Delta \phi)}$$
 (3.2)

It represents the correlation distribution function of the same event *i.e.* associated yield per trigger particle in the same event, normalised by the number of trigger particles. Here, the trigger and associated particles are chosen from the same event.

 $B(\Delta \eta \Delta \phi)$  is given as:

$$B(\Delta \eta \Delta \phi) = \frac{d^2 N_{mixed}^{pair}}{d(\Delta \eta \Delta \phi)}$$
 (3.3)

It represents the correlation distribution function of the mixed event i.e. associated yield per trigger particle in the mixed event. The trigger and associated particles in this case are chosen from different events. The factor B(0,0) in equation (3.1) is chosen so as to normalise the

mixed-event correlation such that it is unity for pairs of particles going in approximately the same direction i.e.  $(\Delta \eta, \Delta \phi) \approx (0,0)$ .

In order to understand how the system collectivity expands, we fit the correlation function with a Fourier expansion series, which gives information about the various flow coefficients.

In order to do this, we first take a projection of equation (3.1) onto the  $\Delta \phi$  axis in the intervals of  $\Delta \eta$  i.e.

$$\frac{dN}{d(\Delta\phi)}|_{a,b} \equiv \int_{|\Delta\eta| \in [a,b]} d\Delta\eta \frac{d^2 N^{pair}}{d(\Delta\eta\Delta\phi)}$$
(3.4)

we then fit equation (3.4) with a Fourier expansion, whose coefficients are the magnitudes of various type of flow and thus they describe the momentum-space anisotropy.

$$\frac{1}{N_{trig}} \frac{dN^{pair}}{d(\Delta\phi)} \propto \left[1 + \sum_{n=1}^{\infty} 2v_n \cos(n\Delta\phi)\right]$$
 (3.5)

Here,  $v_n$  are the Fourier coefficients, where  $v_1$  represents directed flow;  $v_2$  represents elliptic flow and so on.

#### 3.1 Event generation and Analysis methodology

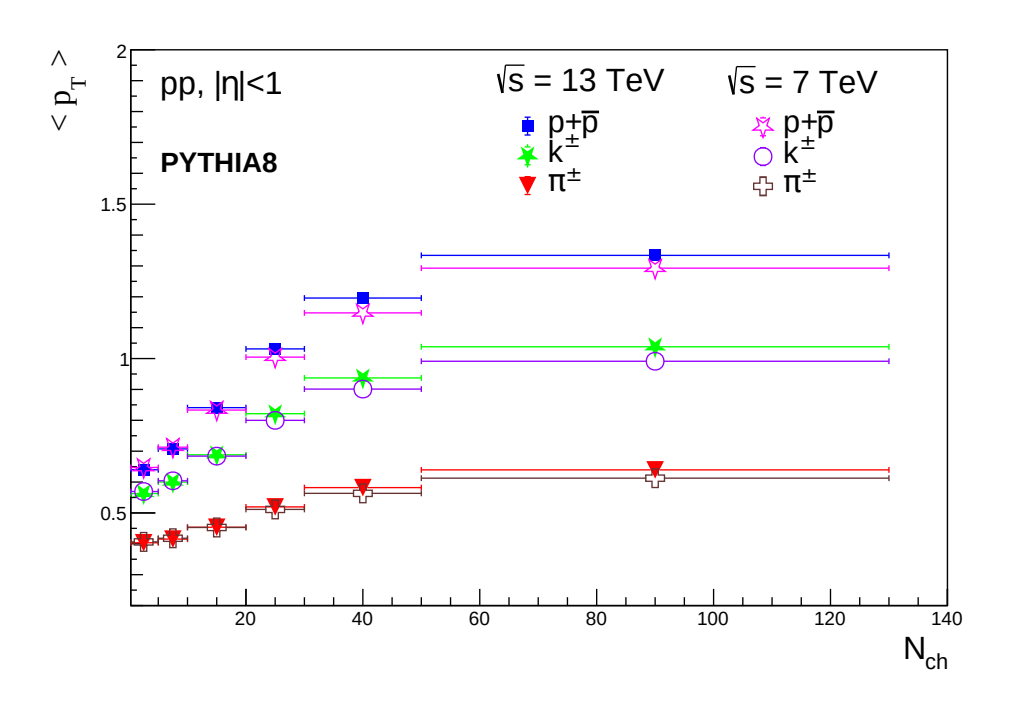
We have chosen pp collisions at LHC energies as the system for our analysis. Our analysis is complex in nature involving multiple steps, starting from data generation (event generation) and storing them in pointers (nTuples) according to our specific needs, then followed by analysing those stored data in order to extract relevant physics information. Using PYTHIA8 event generator, we generated 40 million event in pp collision  $\sqrt{s}=13$  TeV and 7 TeV, and carried out the analysis within CERN based ROOT framework. We have used 4C tuned of PYTHIA8 (Tune:pp=5) and simulated inelastic, non- diffractive component of the total cross section for all hard QCD processes by using the flag "HardQCD:all = on". We have considered the contribution of underlying events like multi-parton interactions (MPIs) by using the flag "PartonLevel:MPI=on" along with MPI-based scheme of color reconnection (CR) mechanism via "ColorReconnection:reconnect = on" in which the color flow of two systems can be fused, by the addition of the partons of the lower- $p_{\rm T}$  system with the strings of the higher- $p_{\rm T}$  system to give the smallest total string length. MPI and CR are considered to see the effect of thermalised medium in this analysis. To study correlation between hadrons and charged-particles, trigger particle and associated particles at the midrapidity  $(|\eta| < 1)$  are considered. The trigger particles chosen for this analysis are charged pion, kaon and proton and all other charged hadrons as associated particles. The trigger particles are chosen in a way such that they have the highest  $p_{\rm T}$  in the event and the associated particles have  $p_{\rm T} > 0.5~GeV/c$ .

### Chapter 4

## Analysis and Discussion

# 4.1 Mean Transverse Momentum and Charged-Particle Multiplicity

Our analysis starts by obtaining the mean transverse momentum  $(\langle p_T \rangle)$  with respect to the charged multiplicity for charged pions  $(\pi^{\pm})$ , kaons  $(k^{\pm})$  and protons and charged multiplicity distribution as show in Figure 4.1. We see that the  $\langle p_T \rangle$  in Figure 4.1 (left) increases and eventually gets saturated, as we proceed from low multiplicity to high multiplicity events. This strong increase in  $\langle p_T \rangle$  is due to color reconnection between strings produced in multi-partonic interaction. From Figure 4.2, we can see that MPI saturates at high multiplicity events and due to this incoherent superposition of large number of MPIs,  $\langle p_T \rangle$  gets saturated as well. This gives us an idea about the importance of MPI as we proceed towards high multiplicity events. One of the major goals of this work is to see the dynamics of pp system with multiplicity. To achieve this, we have considered different multiplicity classes



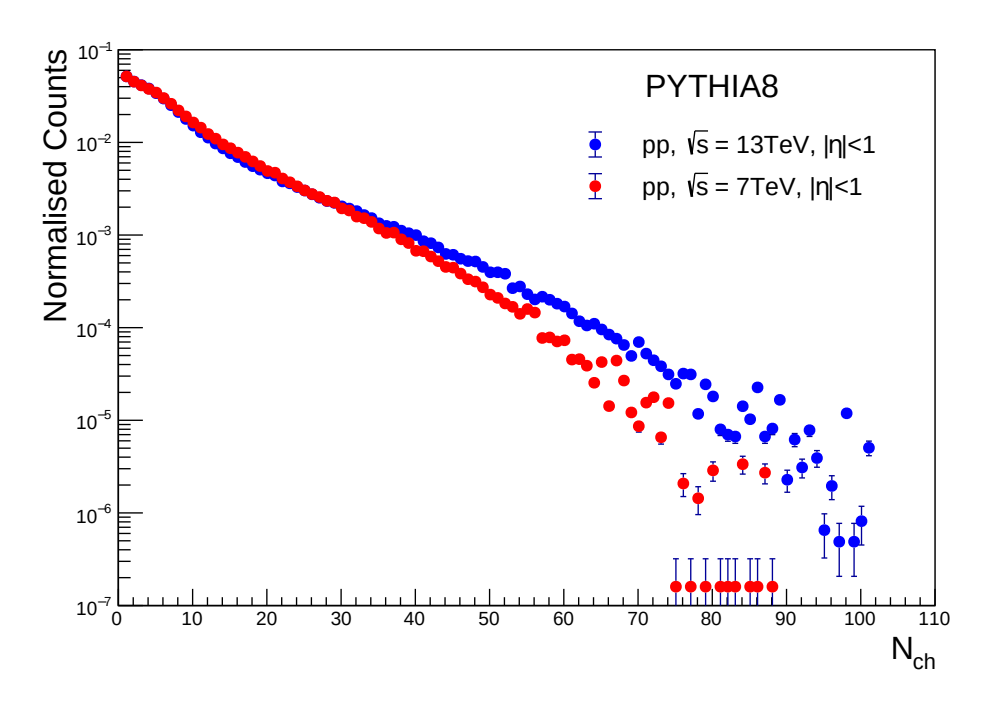


Figure 4.1: (Color Online) (Top) Mean Transverse momentum  $< p_T > \text{vs } N_{ch}$  (Bottom) Charged Multiplicity distribution for pp collision at  $\sqrt{s}=13~$  TeV and 7 TeV

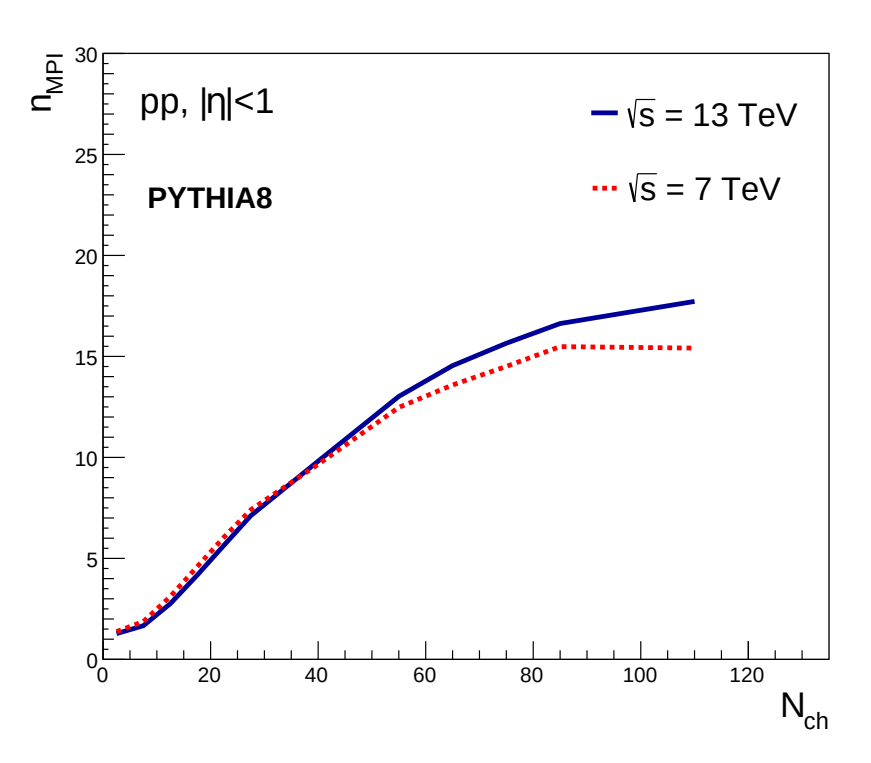


Figure 4.2: (Color Online) number of Multi Partonic Interaction  $(n_{MPI})$  vs  $N_{ch}$ . We can see that  $n_{MPI}$  gets saturated at high multiplicity

from the charged-particle multiplicity distribution as shown in Figure 1.6. The following table shows the different multiplicity classes chosen for our analysis:

Multiplicity class	1	2	3	4	5	6
$N_{ch}$	0-5	5-10	10-20	20-30	30-50	50-130

Table 4.1: Event multiplicity classes used in the analysis. It may be noted here that the analysis has been performed within midrapidity range  $|\eta| < 1$ .

# 4.2 Two-dimensional $(\Delta \eta - \Delta \phi)$ correlation distribution

Now, we proceed with the correlation distribution for the correlation function (Equation 3.1) in the same event and mixed event. This is done by forming pairs of particles in each event by associating the trigger particle with the associated particles (charged hadrons) in terms of their differences in the azimuthal angle ( $\Delta \phi = \phi_{trig} - \phi_{assoc}$ ) and pseudorapidity ( $\Delta \eta = \eta_{trig} - \eta_{assoc}$ ), thereby obtaining the correlation function for the three charged particles (pion, kaon and proton). Here, we correct the raw correlation function by mixed event technique, in which we divide the correlation distribution of the same event by the mixed event bin-wise. The distribution is then normalised by a constant factor B(0,0), which is obtained in such a way that the distribution of mixed event is unity for pairs of particles going in approximately the same direction i.e.  $\Delta \eta \approx \Delta \phi \approx 0$ . This particular normalization in hadron-hadron correlation is adopted with the consideration that the trigger particle and associated particles experience the same detector effect at  $\Delta \eta \approx \Delta \phi \approx 0$ .

Figure 4.3 and 4.4 and Figure 4.5 and 4.4 represent the two-dimensional  $(\Delta \eta - \Delta \phi)$  correlation function for charged pion  $(\pi^{\pm})$ , kaon  $(k^{\pm})$  and proton at  $\sqrt{s} = 13$  TeV and  $\sqrt{s} = 7$  TeV, respectively. As expected, we observe a sharp correlation peak at the near-side  $(\Delta \phi \approx 0)$ , for both low and high multiplicities for all the three trigger particles at both  $\sqrt{s} = 13$  TeV and  $\sqrt{s} = 7$  TeV. This sharp peak is

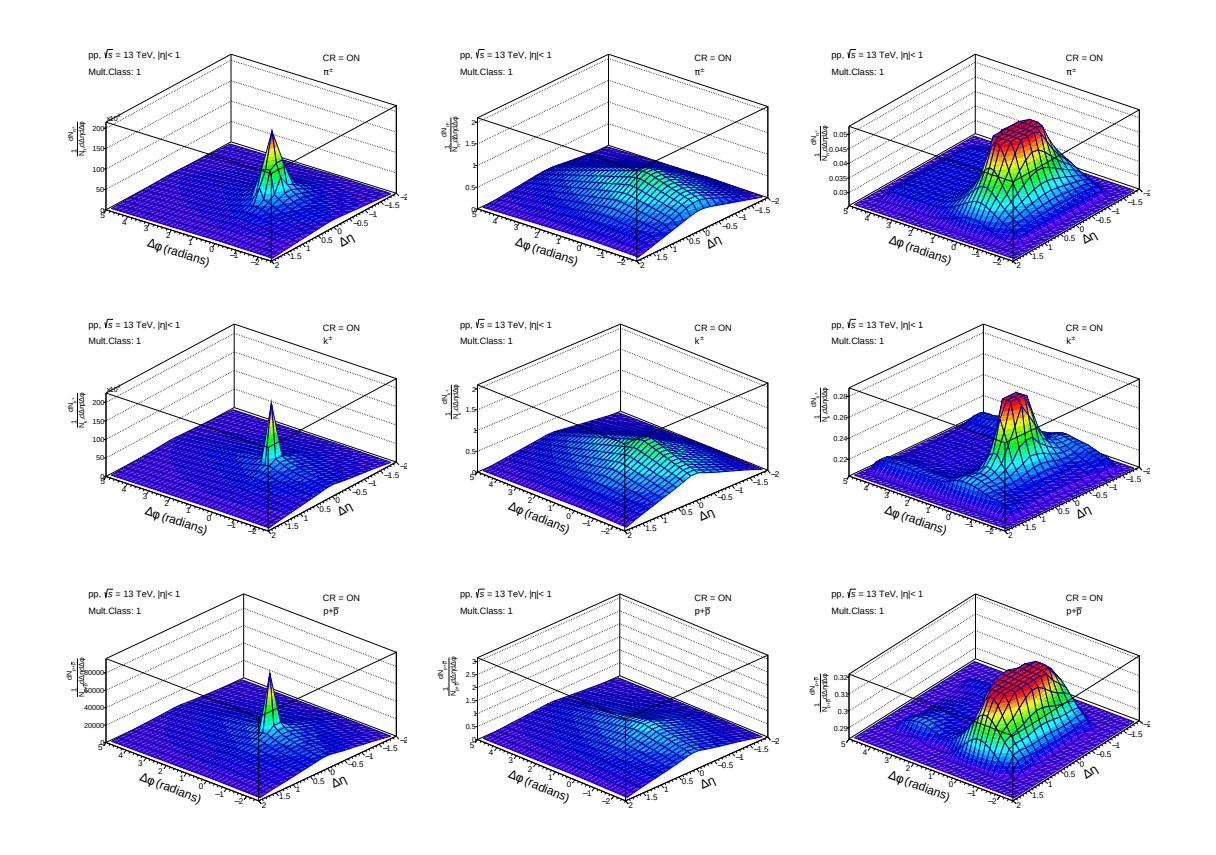


Figure 4.3: (Color Online) Column (I) Correlation distributions for same event, Column (II) Correlation distributions for mixed events, Column (III) Ratio of same event correlation distribution to mixed event correlation distribution for low multiplicity (Mult.Class: 1) at  $\sqrt{s} = 13$  TeV for Pion  $(\pi^{\pm})$  [Row(I)], Kaon $(k^{\pm})$  [Row(II)] and Proton [Row(III)]

due to the strong correlations between the particles produced from the same parent parton. We also observe a long-range ridge-like structure extending to higher units in  $\Delta\eta$  for both low and high multiplicities at both at both  $\sqrt{s}=13\,$  TeV and  $\sqrt{s}=7\,$  TeV for all the three trigger particles . However, in the away-side  $(\Delta\phi\approx\pi)$  region, this long ridge-like structure is prominent only at high multiplicities. This is true for all the three charged particles at both  $\sqrt{s}=13\,$  TeV and 7 TeV, respectively. It is also apparent that the near-side peak gradually increases as we proceed towards high-multiplicity from low-multiplicity due to the increase in the number of multi-partonic interactions,

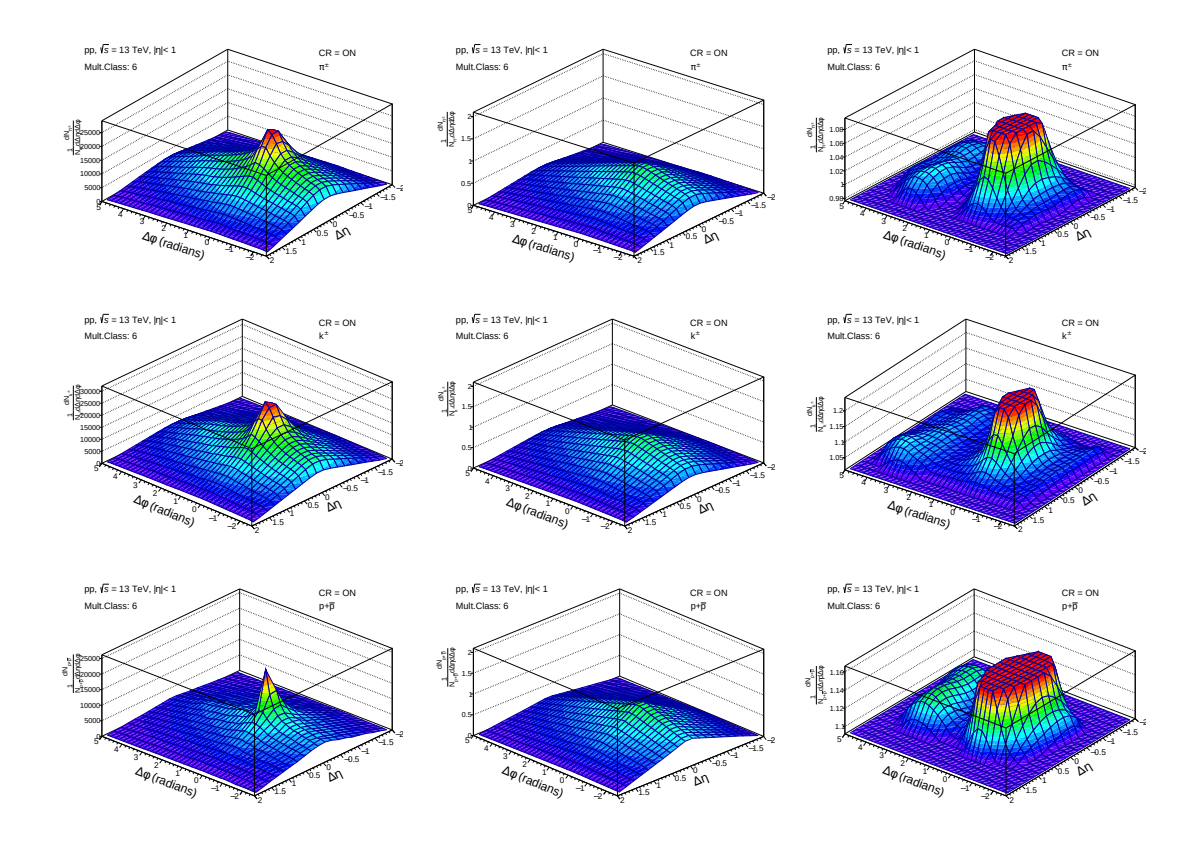


Figure 4.4: (Color Online) Column (I) Correlation distributions for same event, Column (II) Correlation distributions for mixed events, Column (III) Ratio of same event correlation distribution to mixed event correlation distribution for high multiplicity (Mult.Class: 6) at  $\sqrt{s} = 13$  TeV for Pion  $(\pi^{\pm})$  [Row(I)], Kaon $(k^{\pm})$  [Row(II)] and Proton [Row(III)]

indicating that more number of particles are produced from the same jet as compared to the recoiled jets.

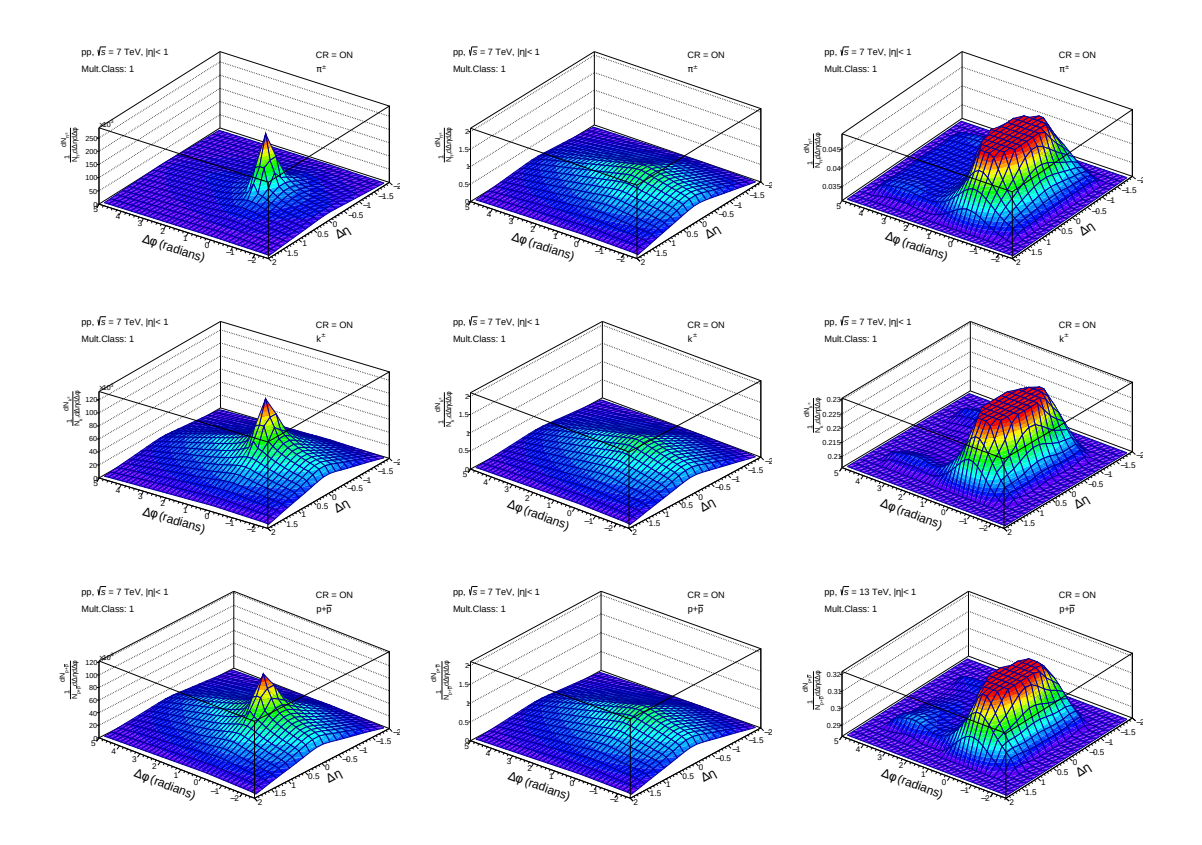


Figure 4.5: (Color Online) Column (I) Correlation distributions for same event, Column (II) Correlation distributions for mixed events, Column (III) Ratio of same event correlation distribution to mixed event correlation distribution for low multiplicity (Mult.Class: 1) at  $\sqrt{s} = 7$  TeV for Pion  $(\pi^{\pm})$  [Row(I)], Kaon $(k^{\pm})$  [Row(II)] and Proton [Row(III)]

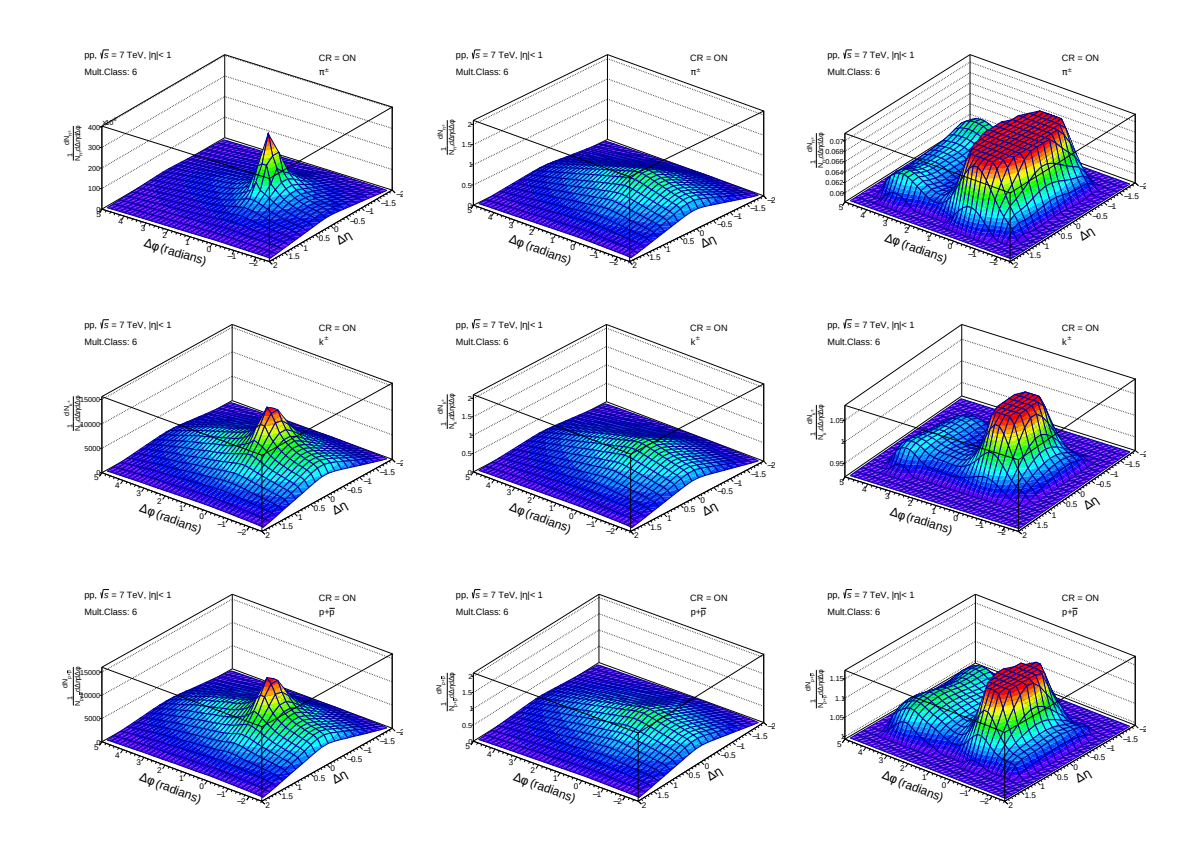


Figure 4.6: (Color Online) Column (I) Correlation distributions for same event, Column (II) Correlation distributions for mixed events, Column (III) Ratio of same event correlation distribution to mixed event correlation distribution for high multiplicity (Mult.Class: 6) at  $\sqrt{s} = 7$  TeV for Pion  $(\pi^{\pm})$  [Row(I)], Kaon $(k^{\pm})$  [Row(II)] and Proton [Row(III)]

#### 4.3 One-dimensional $(\Delta \phi)$ correlation function

As mentioned in the previous chapter, the one-dimensional  $(\Delta \phi)$  correlation function, given by Equation 3.5 is obtained by taking the projection of the two-dimensional  $(\Delta \eta - \Delta \phi)$  correlation function onto the  $\Delta \phi$  axis in the intervals of  $\Delta \eta$  *i.e.* integrating Equation 3.1 over  $\Delta \eta$ .

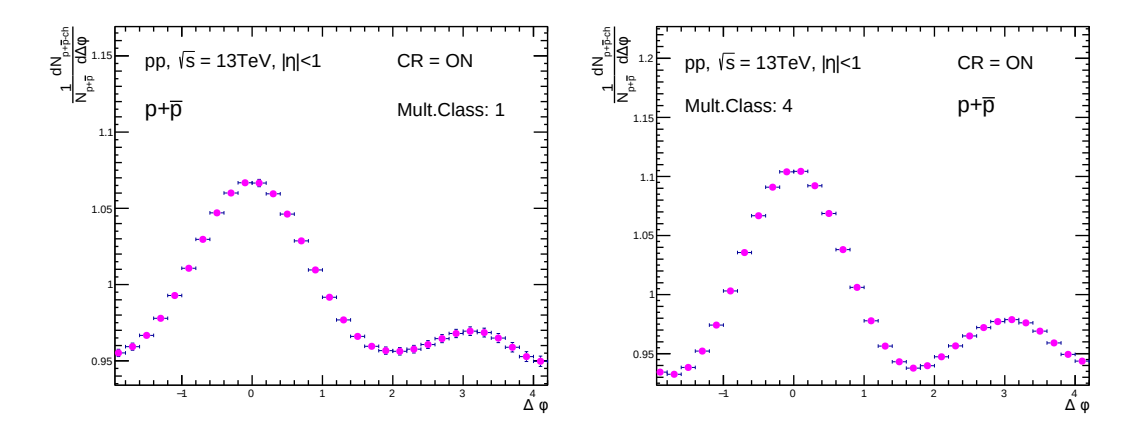


Figure 4.7: Uncorrected 1-D Correlation Distribution of proton for two multiplicity classes. As we can see, the baseline for the two multiplicity classes in comparison is not same

Figure 4.7 shows the uncorrected one-dimensional  $(\Delta \phi)$  correlation distribution for two multiplicity classes. As we can see the initial baseline of the vertical axis is not the same for the two multiplicity classes in comparison. Thus, it is not possible to make a comparison analysis as the two plots do not have the same footing. In order to rectify this, we have used a method in line with ZYAM (Zero Yield At Minimum) [15], as a result of which the minimum of the correlation function has zero associated yield, thereby making the baseline of all the multiplicity classes equal.

Figure 4.8 represents the corrected one-dimensional correlation distribution of charged pion, kaon and proton for minimum bias, low multiplicity (Mult.Class: 1) and high multiplicity (Mult.Class: 6) classes. We can see that the correlation distributions are unique and show peaks at  $\Delta \phi \approx 0$  which we are calling it as the near-side and at  $\Delta \phi \approx \pi$  which is the away-side. The peak around the near-side indicates a strong correlation between the particles produced from the same parent parton, while the peak at the away-side is from the recoiled parton which comes as a consequence of the energy-momentum conservation, whereby it too fragments to produce particles.

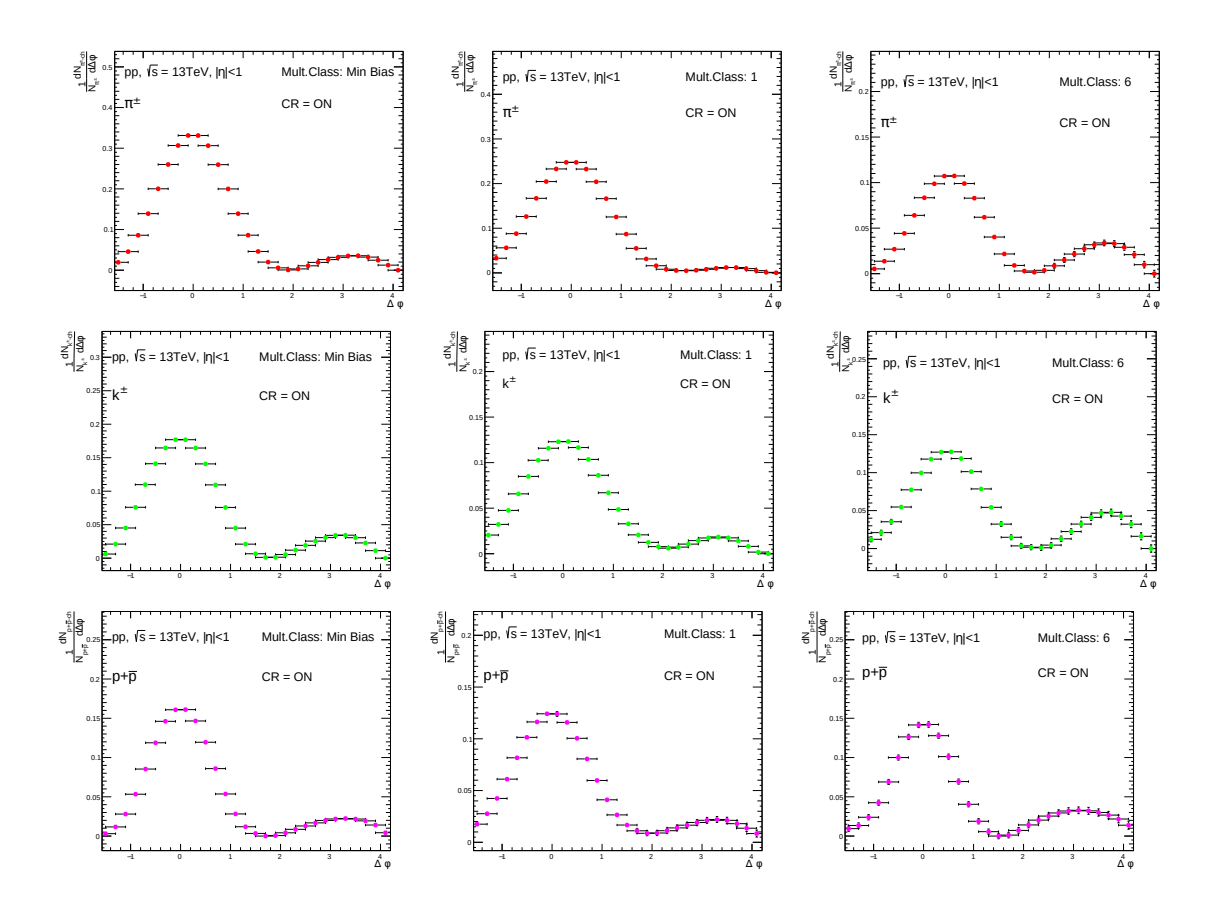


Figure 4.8: (Color Online) Column (I) Corrected 1-D Correlation Distribution for Min. Bias, Column (II) Corrected 1-D Correlation Distribution for low multiplicity (Mult. Class: 1), Column (III) Corrected 1-D Correlation Distribution for high multiplicity (Mult.Class: 6)

The suppression of peak on the away-side is due to the fact that the recoiled parton traverses more path in the medium thereby its interaction with the medium increases and hence loses more energy. The other entries in the histogram reflect the complexity of the underlying events in the strong interactions, where many other particles are produced from the fragmentation of other partons.

#### 4.4 Estimation of flow-like effects

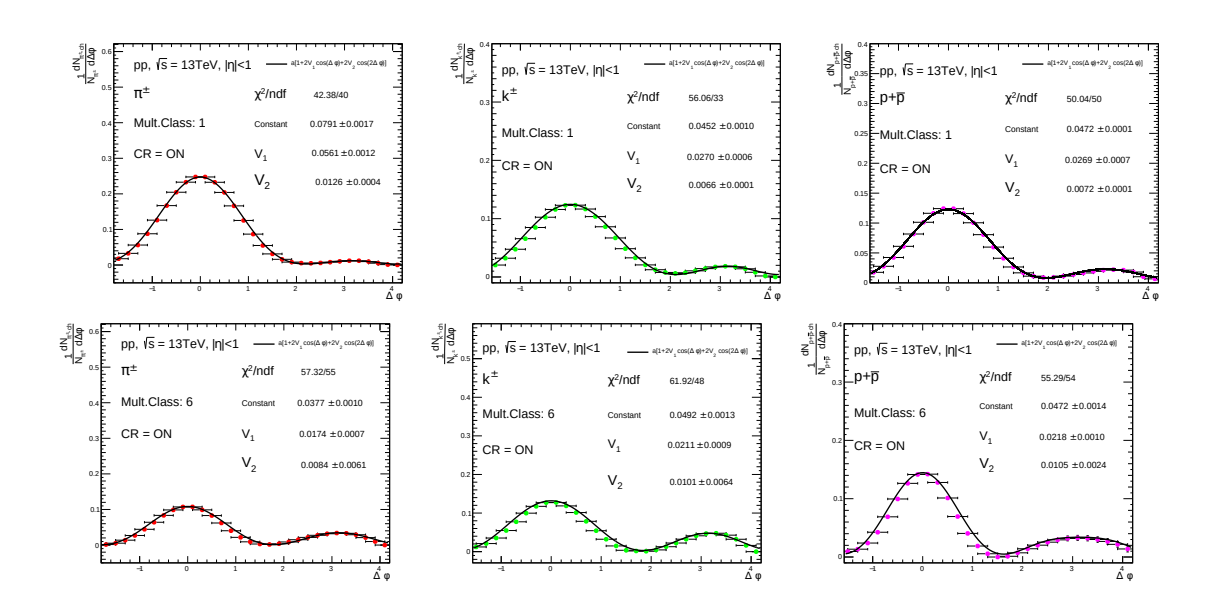


Figure 4.9: (Color Online) Row (I) Fitted correlation distributions for  $\pi^{\pm}$ ,  $k^{\pm}$ ,  $p+\bar{p}$  for low multiplicity class and Row (II) for high multiplicity class

As discussed earlier, we then fitted the obtained one-dimensional correlation function with a Fourier series (Equation 3.5), in order to have an idea about how the system collectivity expands. The coefficients of the Fourier series gives information about the flow coefficients. The second Fourier series coefficient, known as the elliptic flow coefficient  $(v_2)$  gives us an idea of collective flow in the medium. Figure 4.9 shows the fitted correlation distribution for charged pion, kaon and proton for

low and high multiplicity class.

Thus, we have extracted  $v_2$  from our fitted 1-D correlation distribution and plotted it as a function of different charged multiplicity classes.

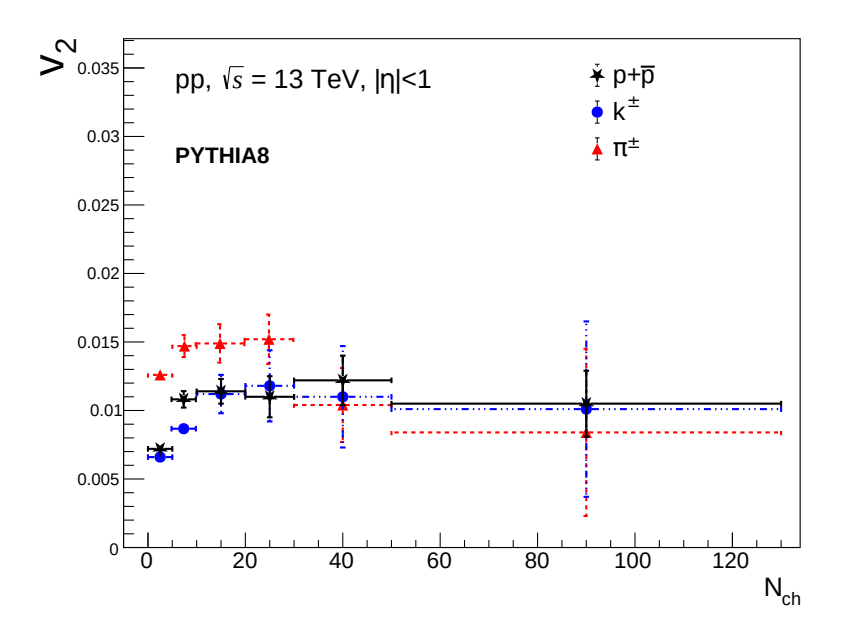


Figure 4.10: (Color Online)  $v_2$  vs.  $N_{ch}$  for  $\pi^{\pm}$ ,  $k^{\pm}$ ,  $p+\bar{p}$ 

Figure 4.10 represents the values of  $v_2$  as a function of charged multiplicities for charged pion, kaon and proton. Here we observe that as we move towards high multiplicity from low multiplicity, the value of  $v_2$  first increases and then gradually decreases for all the three trigger particles. This trend is qualitatively similar to that of the heavy-ion collision (Pb+Pb) at the LHC [16]. The gradual decrease in the value of  $v_2$  as we proceed towards high multiplicity from low multiplicity is due to the fact that high multiplicity classes corresponds to central type of collisions (head-on collision), in which the overlapping region of the two nuclei is more of spherical in shape, rather than elliptical. And as we know, the anisotropic flow is sensitive to initial geometry of the system, hence the magnitude of elliptical flow i.e.  $v_2$  is observed to decrease at high multiplicity (central collisions) events.

#### 4.5 Extraction of relative associated yields

In order to see the variation of medium effects as a function of charged particle multiplicity, we have obtained the relative yield at near-side and away-side for different multiplicity classes and compared it with low multiplicity class. We term this as relative associated yield  $(I_{pp})$ . Its expression is given as:

$$I_{pp} = \frac{(Y_{NS}/Y_{AS})_i}{(Y_{NS}/Y_{AS})_{LM}} \tag{4.1}$$

where  $Y_{NS}$  and  $Y_{AS}$  are the yields of the near and away-side, which is obtained by integrating the fitted one-dimensional  $\Delta \phi$  correlation distribution over a region  $|\Delta \phi| < 0.7$  for near-side and  $|\Delta \phi - \pi| < 0.7$  for the away-side respectively. Here "i" denotes the multiplicity bin.

We have chosen the ratio of near-side to away-side of low multiplicity class (Mult. Class: 1) as our baseline since at low multiplicity we do not expect medium-like formation as seen in our previous results (Figure 4.3 and 4.5).

Figure 4.11 shows the value of  $I_{pp}$  as a function of multiplicity for charged pion, kaon and proton. From Equation 4.11, it is clear that enhancement above unity shows that the particles produced from away-side parton suffers more medium effect. As MPI plays a dominant role towards the high multiplicity events, which leads to an increase in production of particles, hence, it is expected to observe an enhancement of  $I_{pp}$  towards high multiplicity events. It is also worth nothing that  $I_{pp}$  is constant

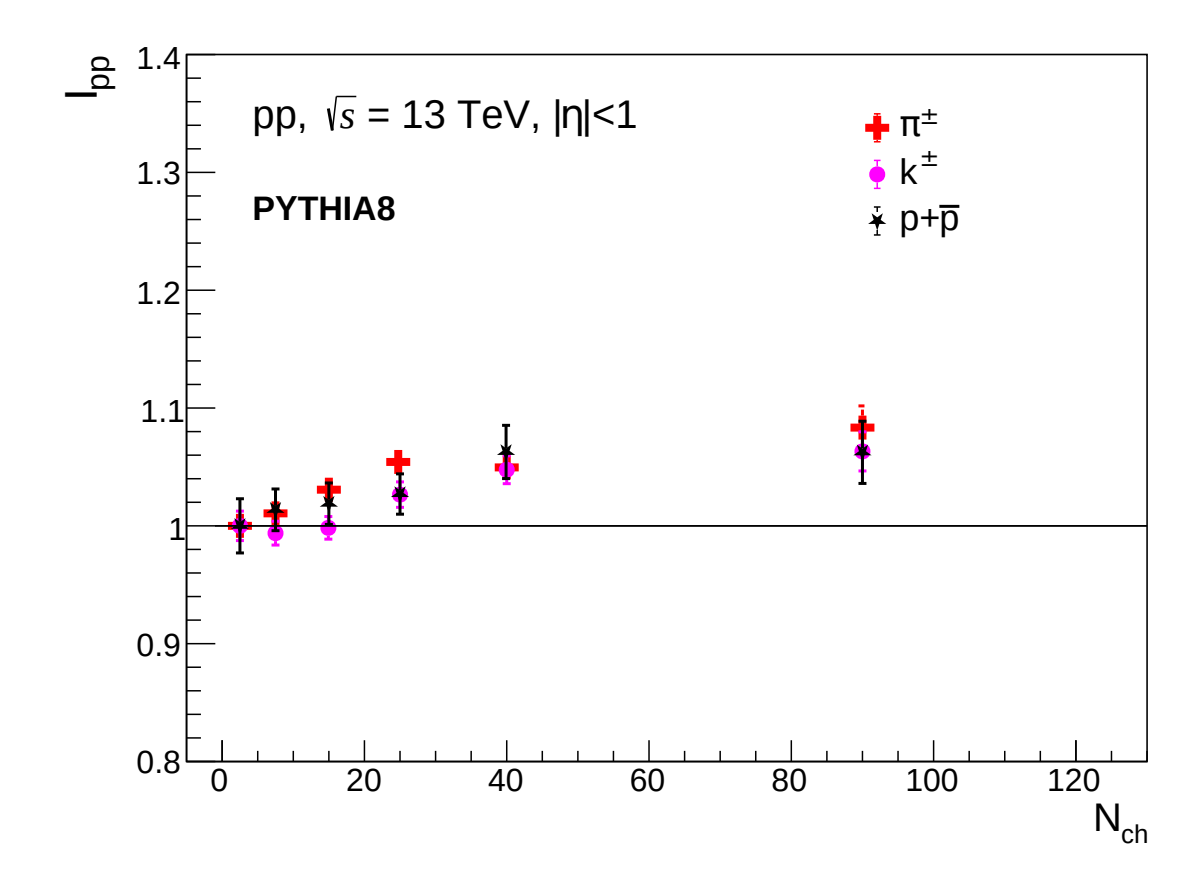


Figure 4.11: (Color Online)  $I_{pp}$  vs.  $N_{ch}$  for  $\pi^{\pm}, k^{\pm}, p+\bar{p}$ 

for long-lived hadrons within uncertainty. This shows that the non-flow effect, like flow-effect, is collective in nature.

### Chapter 5

# Summary and Outlook

In this thesis, we have studied the non-flow effects in pp system by twoparticle correlation method using PYTHIA8. We have considered pion, kaon and proton having the highest  $p_T$  as our trigger particles and all other charged hadrons having  $p_T > 0.5 \text{ GeV/c}$  as our associated particles. Using the two particle correlation method, we then obtained the distribution for the correlation function in the same and mixed events for different charged multiplicity bins and then corrected the raw correlation function by mixed event technique, normalised by a constant factor B(0,0). We further obtained the one-dimensional  $(\Delta \phi)$  correlation distribution over which we fitted a Fourier series, whose second coefficient known as elliptical flow  $(v_2)$  tells us about the anisotropy in momentum space. The values of  $v_2$  is then plotted as a function of different charged multiplicity. Furthermore, in order to see the variation of medium effect on the near-side and away-side as charged multiplicity changes, we have obtained the associated yield, and then plotted it as a function of charged multiplicity.

The following is a summary of the thesis findings:

- 1. We have obtained the  $(\Delta \eta \Delta \phi)$  correlation distribution for charged pion, kaon and proton at both  $\sqrt{s} = 13$  TeV and 7 TeV. We have observed that the long ridge-like structure on the  $\Delta \eta$  axis is visible only for high multiplicity class for all the three trigger particles. This is true for both  $\sqrt{s} = 13$  TeV and 7 TeV. This indicates that the role of Multi Partonic Interaction (MPI) and Color Reconnection (CR) of PYTHIA8, which mimics medium-like effect is prominent towards high multiplicity class.
- 2. On fitting the one-dimensional  $\Delta \phi$  correlation distribution with a Fourier series representing the azimuthal distribution function, its second coefficient  $(v_2)$  tells us about the elliptic flow; we then plotted  $v_2$  as a function of charged multiplicity (Figure 4.10). We have observed that as multiplicity increases, the value of  $v_2$  initially increases, and then decreases gradually. This is true for all the three trigger particles. This indicates that elliptic flow for individual light particles qualitatively behaves like elliptic flow in heavy-ion collisions.
- 3. In order to see medium effect, we have calculated relative associated yield  $(I_{pp})$ . We have kept low multiplicity as our baseline, since the effect of MPI+CR does not seem to have a prominent role at low multiplicity. From the  $I_{pp}$  vs  $N_{ch}$  plot, we see that  $I_{pp}$  for all the three long-lived hadrons have an enhancement above unity for all multiplicity classes thereby suggesting that the particles produced from back-to-back jets suffer more medium effects. It is also

worth nothing that  $I_{pp}$  is constant for long-lived hadrons within uncertainty. This shows that the non-flow effect, like flow-effect, is collective in nature.

The results obtained through these work tells us that the behaviour of elliptical flow for individual particles is different as opposed to studying the elliptical flow of the charged particles altogether. Since PYTHIA gives purely non-flow  $v_2$ , one can use this results as a filter to the actual LHC data, so as to obtain the real flow signal.

## Bibliography

- [1] Quantum Diaries, URL: https://www.quantumdiaries.org.
- [2] URL: https://www.bnl.gov/newsroom/news.php?a=24281.
- [3] R. Sahoo, AAPPS Bull. **29**, 16 (2019).
- [4] R. Sahoo, arXiv:1604.02651.
- [5] URL: https://tikz.net/axis2d\_pseudorapidity/
- [6] Ashish Bisht, M.Sc. Thesis, IIT Indore, (2019).
- [7] R. Snellings, New J. Phys. **13**, 055008 (2011).
- [8] T. Niida and Y. Miake, AAPPS Bull. **31**, 12 (2021).
- [9] J. Adam et al. [ALICE Collaboration], Nature Phys. 13, 535 (2017).
- [10] T. Sjöstrand, S. Ask, J. R. Christiansen, R. Corke, N. Desai, P. Ilten, S. Mrenna, S. Prestel, C. O. Rasmussen and P. Z. Skands, Comput. Phys. Commun. 191, 159 (2015).
- [11] R. Brun and F. Rademakers, Nucl. Instrum. Meth. A 389, 81 (1997).
- [12] D. Velicanu [CMS Collaboration], J. Phys. G 38, 124051 (2011).

- [13] J. Adam *et al.* [ALICE Collaboration], Phys. Lett. B **763**, 238 (2016).
- [14] S. Kar, S. Choudhury, S. Muhuri and P. Ghosh, Phys. Rev. D 95, 014016 (2017).
- [15] N. N. Ajitanand, J. M. Alexander, P. Chung, W. G. Holzmann, M. Issah, R. A. Lacey, A. Shevel, A. Taranenko and P. Danielewicz, Phys. Rev. C 72, 011902 (2005).
- [16] B. Schenke, C. Shen and P. Tribedy, Phys. Rev. C 102, 044905 (2020).